Chemical Engineering Journal 174 (2011) 102–109

Contents lists available at SciVerse ScienceDirect

Chemical Engineering Journal

journal homepage: www.elsevier.com/locate/cej

Drinking water treatment in a gravimetric flow system with TiO_2 coated membranes

Rosângela Bergamasco[a,*], Flávia Vieira da Silva[a], Flávia Sayuri Arakawa[a], Natália Ueda Yamaguchi[a], Miria Hespanhol Miranda Reis[b], Carlos J. Tavares[c], Maria Teresa Pessoa Sousa de Amorim[d], Célia Regina Granhen Tavares[a]

[a] State University of Maringá, Chemical Engineering Department, Av. Colombo, 5790, Zip Code: 87020-900, Maringá, PR, Brazil
[b] Federal University of Uberlândia, Chemical Engineering Department, Av. João Naves de Ávila, 2121, Zip Code: 38400-902, Uberlândia, MG, Brazil
[c] Minho University, Departamento de Física, GRF, 4800-058 Guimarães, Portugal
[d] Minho University, Departamento de Engenharia Têxtil, Centro de Ciência e Tecnologia, Campus Azurém, Guimarães, Portugal

ARTICLE INFO

Article history:
Received 20 April 2011
Received in revised form 18 August 2011
Accepted 19 August 2011

Keywords:
Drinking water
Membrane modification
TiO_2 film
Membrane fouling

ABSTRACT

This paper presents filtration results for drinking water treatment obtained with a commercial cellulose acetate membrane of 0.45 μm pore diameter, with and without TiO_2 coating. The deposition of titanium dioxide thin films onto membrane surface was made by pulsed-frequency d.c. reactive magnetron sputtering at room temperature from a high purity Ti target in $Ar/O_2/N_2$ atmosphere, at different conditions for cathode current and for deposition time. The proposed membranes were used in a filtration system driven by gravitation without the requirement of energy supply. The obtained results showed that the proposed system is able to remove color and turbidity from raw water. Besides, the modified membrane presented better results than the neat one regarding to membrane fouling and chlorine removal.

1. Introduction

The accessibility of safe and suitable drinking water is an important factor to decrease the mortality due to waterborne diseases. The World Health Organization (WHO) related that approximately half of population from developing countries has health problems related to the lack of suitable drinking water access or to the presence of microbiological contamination in water [1]. Diarrhoeal diseases, due to bacterial, viral, and parasitic agents of gastroenteritis and viral hepatitis are the most important groups of water-related infections and are a leading cause of childhood morbidity and mortality [2].

Nowadays, membrane separation processes have been cited as a suitable process for water treatment, since they can provide an absolute barrier for bacteria and viruses, besides removing turbidity and color [3]. Although the costs of membranes have decreased during the last decade, this technology is not yet broadcasted worldwide, especially for poorest communities [4].

Most membrane processes requires pumps to promote the trans-membrane pressure, resulting in energy consumption and relative high costs of auxiliary equipments. Alternatively, membrane processes can be designed to operate at low pressures with gravity acting to promote the driven-pressure. In addition to concerns over microbial contaminant removals, low-pressure membranes are becoming more attractive due to some other reasons, such as stricter regulatory requirements, operation easiness, minimum staffing requirements, competitive cost and independence of water source quality [5]. On the other hand, this applied low pressure may result in low permeate fluxes. In this way, the process must be properly designed in order to obtain the desired flux, looking for suitable membrane material and configuration.

Huang et al. [6] highlighted that the application of low pressure membrane technologies for water treatment is growing since the beginning of the above decade. Peter-Varbanets et al. [7] listed a few known membrane processes that use gravity as the driven force for water treatment, such as the LifeStraw Family from Vestergaard Frandsen. Vestergaard Fransen S.A. (Lausanne, Switzerland) is a European-based international company that developed a point-of-use system consisting of ultrafiltration capillary membranes that are placed at an elevated level to create a pressure of 100–150 mbar [8].

Essentially, fouling is a major constraint during separation using membranes. Its occurrence leads to a decline in membrane permeability and can occur either by the deposition of a new layer on the membrane surface (cake filtration) or by intermediate, total, or internal pore blocking, besides mechanisms as spacer clogging and adsorptive fouling. Fouling limits membrane process applications,

* Corresponding author. Tel.: +55 44 3011 4748; fax: +55 44 3011 4792.
E-mail address: rosangela@deq.uem.br (R. Bergamasco).

1385-8947/$ – see front matter © 2011 Elsevier B.V. All rights reserved.
doi:10.1016/j.cej.2011.08.056

since frequent cleaning procedures or even membrane substitutions are required, increasing the required costs. Therefore, it is important to study alternatives to reduce fouling and, at the same time, increase permeability and selectivity of commercial membranes.

Chemical membrane modifications, such as by assembling additional compounds in membrane composition, have been proposed to realize high membrane permeability over a prolonged period of time. Addition of TiO_2 particles on membrane structure and surface has been proposed as an effective method to improve membrane antifouling properties [9,10]. The main interest on TiO_2 is due to its photocatalytic and hydrophilic effects. Wang et al. [11] investigated the application of a proton exchange membrane (Nafion 117) with TiO_2 in a photoelectrocatalytic process to treat textile wastewater, showing that the application of Nafion as a solid electrolyte is a promising alternative for waste treatment. Chin et al. [12] also showed that a low-pressure submerged membrane photocatalytic reactor is an effective way to purify water containing bisphenol-A. Likodimos et al. [13] emphasized the potential of composite membranes with photocatalytic properties for enhancing water quality.

Some different techniques can be applied to entrap TiO_2 in polymeric membrane matrix or to deposit TiO_2 on membrane structure and surface [14]. Most of the proposed processes apply the phase inversion technique to produce hybrid polymeric membrane adding a known amount of TiO_2 in the main solution. This mixture is then precipitated in a solvent solution. An alternative procedure is to dip the neat polymeric membrane into a TiO_2 solution [15]. Rahimpour et al. [10] showed that coating TiO_2 onto membrane surface is a superior method compared to entrapping TiO_2 particles in the membrane matrix. The former option enables higher permeate fluxes and smaller membrane resistances.

An effective way to immobilize TiO_2 on a substrate must be applied in order to minimize the trade-off between the particle recovery and the mass transfer effectiveness. Pulsed magnetron sputtering is widely recognized as an enabling technology, particularly for the deposition of dielectric materials. Marques et al. [16] applied the unbalanced d.c. pulsed reactive magnetron sputtering method to produce titania films. These films developed very good photocatalytic efficiency by degrading a chosen organic pollutant (C.I. Reactive Blue 19) via irradiation with UV-A light. Tavares et al. [17] also suggested the preparation of TiO_2 thin film by unbalanced reactive magnetron sputtering on a polycarbonate support. The obtained composite films showed improved photocatalytic efficiencies.

The aim of this paper is to investigate the separation capability of a conventional cellulose acetate membrane modified with TiO_2, with respect to permeation water flux and selectivity. The tests were carried out in a low pressure system, proposing a simple module that ensures water quality for human consumption.

2. Material and methods

2.1. Membrane modifications

Flat cellulose acetate microfiltration membranes (pore diameter = 0.45 μm, membrane surface area = 3.36×10^{-3} m^2) were purchased from Advantec (Japan). Titanium dioxide films were deposited onto membrane surfaces by the pulsed-frequency d.c. reactive magnetron sputtering method at room temperature as proposed by Tavares et al. [17]. A schematic representation of the reactive magnetron sputtering method is presented in Fig. 1. The electric field generated by the V_{dc} power supply will ionize the argon (working) gas, accelerating the Ar^+ ions towards the target and subsequently ejecting the neutral Ti atoms that will react with oxygen and condense on the substrate surface as a thin film of TiO_2.

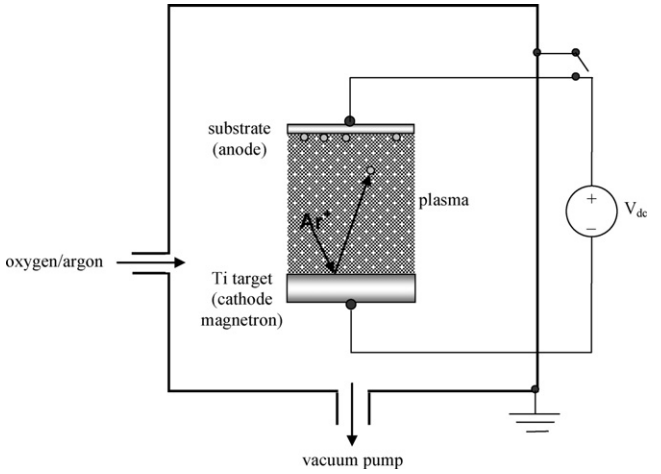

Fig. 1. Reactive magnetron sputtering diagram.

A high purity Ti target in $Ar/O_2/N_2$ atmosphere was applied, varying the cathode current and the deposition time, as shown in Table 1. Neat membrane is identified as M, while the modified membranes are identified as M01, M02, and M03. Sample rotation speed was fixed at 18 rpm. The sputtering process parameters were chosen as starting values based on previous work performed for the deposition of photocatalytic TiO_2 thin films on glass [18] and PVDF [19] surfaces, using the same sputtering source.

Morphological differences between neat and modified membranes were analyzed using SEM (Scanning Electron Microscopy) technique in a scanning electron microscope FEI (model Nova 200 NanoSEM) at magnification of 10,000×.

2.2. Membrane separation system

The proposed membranes were evaluated in filtration system working with gravity to promote the driven force. This system has a main tank with capacity of 20 L to store the water to be filtrated, which supplies the feed tank. Additionally, there is an overflow to keep constant the level of raw water. Feed tank is placed at a particular height from the filtration module corresponding to the required pressure. In this work, tests were carried out at 30397.5 Pa (3.1 m of water column). The flat membrane is fixed at the bottom of the filtration module. Effective membrane surface area is 1.962×10^{-3} m^2. Permeate is collected perpendicularly to the membrane area, by means a dead-end operation.

The proposed low-pressure membrane system was evaluated with neat and modified membranes. Five experiments were done independently, without any clean procedure between these steps.

(1) Determination of initial permeate flux of deonized water with a clean membrane.
(2) Filtration of deionized water artificially contaminated with *Escherichia coli* at 1.0×10^5–1.0×10^6 CFU/100 mL.
(3) Four subsequent filtrations of tap water during 120 min each one, totalizing 480 min of filtration.
(4) Second filtration of water artificially contaminated with *E. coli*, as described in step (2). This test was carried out to evaluate

Table 1
Conditions of titanium dioxide deposition onto membranes surface.

Membrane	Cathode current (A)	Deposition time (h)
M01	0.50	6
M02	0.35	8
M03	0.30	5

membrane efficiency for *E. coli* removal after tap water filtration.

(5) Determination of final permeate flux of deionized water with a dirty membrane.

These steps were chosen in order to analyze the suitability of the proposed process to treat bacteriological contaminated and tap waters and to be used as a household filter.

At the end of each experiment, the filtration module was depressurized, disconnected of the system, and stored with deionized water. This procedure was carried out in order to empty the module and the connected lines for the next filtration with another kind of water. The used membrane was not removed from the module during this procedure.

2.3. Water samples and analysis

Two types of water were used in this work: deionized water artificially contaminated with *E. coli* and tap water from Maringa city (Brazil).

An agar plate diffusion procedure was used to prepare deionized water artificially contaminated with *E. coli*. A standard culture of *E. coli* was enriched in a nutrient broth during 20–22 h. A bacterial suspension was prepared from this enriched culture to a turbidity equal to 0.5 of tube #1 in the MacFarland scale using sterile isotonic saline solution. The standardized inocula were spread over the surface of 15 cm Petri dishes containing 6 mm of Mueller–Hinton agar using sterile cotton swabs. After 15 min of pre-diffusion, 15 mg of the prepared sample was placed over the seeded agar plates. The plates were then incubated at 37 °C during 20–22 h and the diameters of the inhibition zones were measured. These assays were done in duplicate.

After the filtration of contaminated water, E. *coli* removal was evaluated using the membrane filter technique for members of coliform group, as described in Standard Methods for the Examination for Water and Wastewater [20].

The characteristics of the tap water available at Chemical Engineering Faculty (Maringá-Brazil) are: pH 7.8, color = 4.93 UC, and turbidity = 1.15 NTU. Residual chlorine concentration in this tap water was adjusted to 1.5 mg/L using a solution of 14.0 wt% of sodium hypochlorite.

Removal of color, turbidity, and free chlorine, pH variation, and total volume of filtrated were measured after tap water filtration. Turbidity and color were measured with a Hach 2100N turbidimeter and with a Hach DR-A colorimeter, respectively. Free chlorine residuals were measured using a HACH DR/4000 spectrophotometer.

2.4. Membrane resistance analysis

Resistances due to different fouling mechanisms were determined in order to investigate the fouling behavior. Resistances were calculated following the resistance-in-series model adapted from Schafer et al. [21] as presented in Eq. (1):

$$J = \frac{\Delta P}{\eta(R_m + R_p + R_c)} \quad (1)$$

where J is permeate flux [kg m^{-2} s^{-1}], ΔP is trans-membrane pressure [kg m^{-1} s^{-2}], η is dynamic viscosity [kg m^{-1} s^{-1}], and R denotes a resistance [m^2 kg^{-1}]: R_m is membrane hydraulic resistance, R_p is resistance due to pore blocking, and R_c is resistance due to cake formation.

Each resistance was experimentally measured in the gravitational system with neat and modified membranes. Membrane hydraulic resistance (R_m) was determined measuring the flux of deionized water through a clean membrane sheet. In this case, the others resistances are equals to zero.

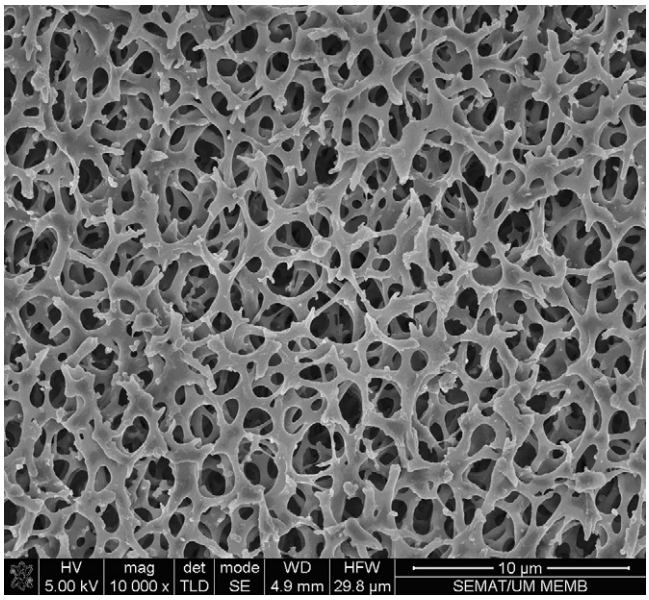

Fig. 2. SEM image of the neat membrane (M).

The sum of resistances due to pore blocking and cake formation ($R_p + R_c$) was determined measuring the flux of deionized water with the fouled membrane, i.e. with the membrane that was used for raw water filtrations without clean procedures.

After that, the fouled membrane was gently cleaned with a sponge to remove the cake layer from the surface. Deionized water was then filtered once again through this same membrane sheet to obtain the resistance due to pore blocking (R_p) [22].

Membrane fouling percentage (%F) was calculated according to Eq. (2), as proposed by Balakrishnan et al. [23]. This percentage represents the drop in deionized water flux after filtration tests with raw water.

$$\%F = \frac{(J_i - J_f)}{J_i} \times 100 \quad (2)$$

where %F is membrane fouling percentage, and J_i and J_f [kg m^{-2} s^{-1}] are deionized water fluxes in clean and fouled membranes, respectively.

3. Results and discussions

3.1. SEM images

SEM images of all the evaluated membranes are shown in Figs. 2–5.

SEM images of the membranes M01, M02, and M03 (Figs. 3–5) show that there is a deposited material on the membrane surface probably due to the presence of TiO_2. Similar results were observed by Syafei et al. [24]. Marques et al. [16] also observed that the TiO_2 deposition increases the occurrence of isotropic spherulites.

This deposited material is more evident in Fig. 4, related to the membrane M02 which was produced at the highest deposition time and at low cathode current. Lee et al. [25] analyzed the effects of pulse frequency and substrate bias on mechanical properties of chromium nitride coatings deposited on silicon wafer substrates by pulsed d.c. magnetron sputtering and observed that the grain size decreases with the increasing of pulse frequency and substrate bias.

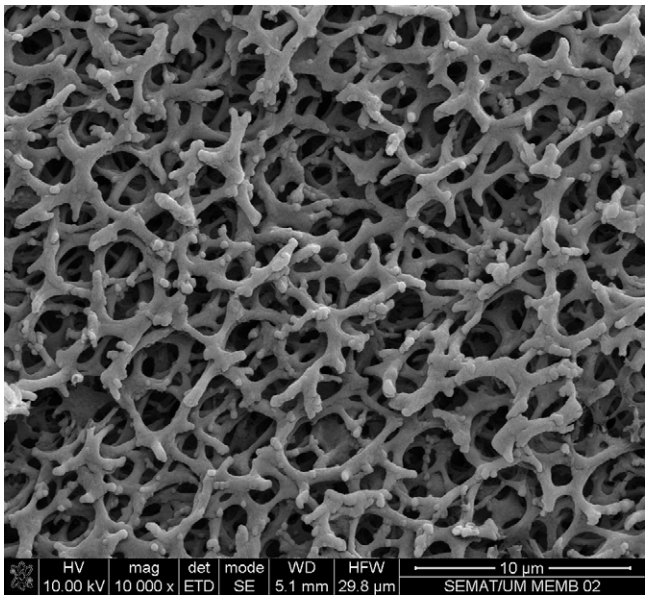

Fig. 3. SEM image of the modified membrane (M01).

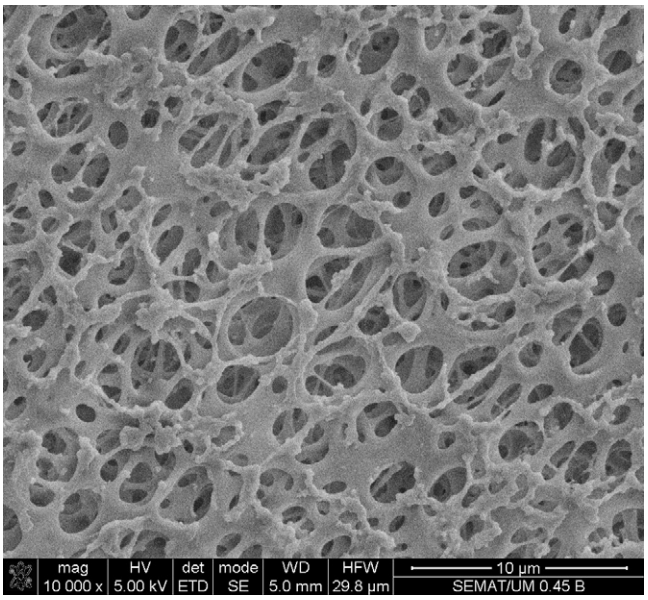

Fig. 5. SEM image of the modified membrane (M03).

3.2. Permeate fluxes

The permeate flux data of deionized water through the clean membranes (step 1 described in Section 2.3) is presented in Fig. 6. The neat membrane (M) presented higher permeate fluxes, followed by the membranes M03, M01, and M02, indicating that higher deposition times induce lower fluxes. A longer deposition time inevitably induces a rougher membrane surface which may decrease the flux of clean water.

Fig. 6(b) presents the flux behavior of all the proposed membranes regarding to the filtrated volume of deionized water. This figure confirms the superior performance of the neat membrane (M) as a clean sheet to filtrate clean water. Comparing the modified membranes, the membrane M03 filtrated more deionized water than the membranes M01 and M02, at the same filtration time, as presented in Fig. 6(b).

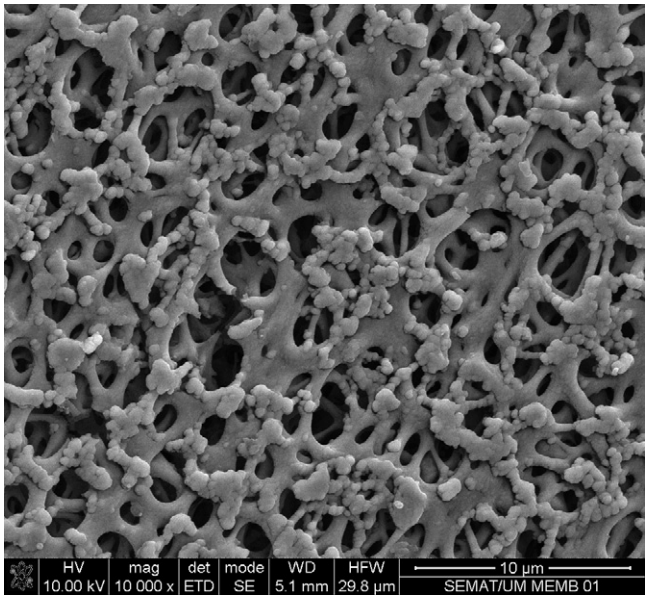

Fig. 4. SEM image of the modified membrane (M02).

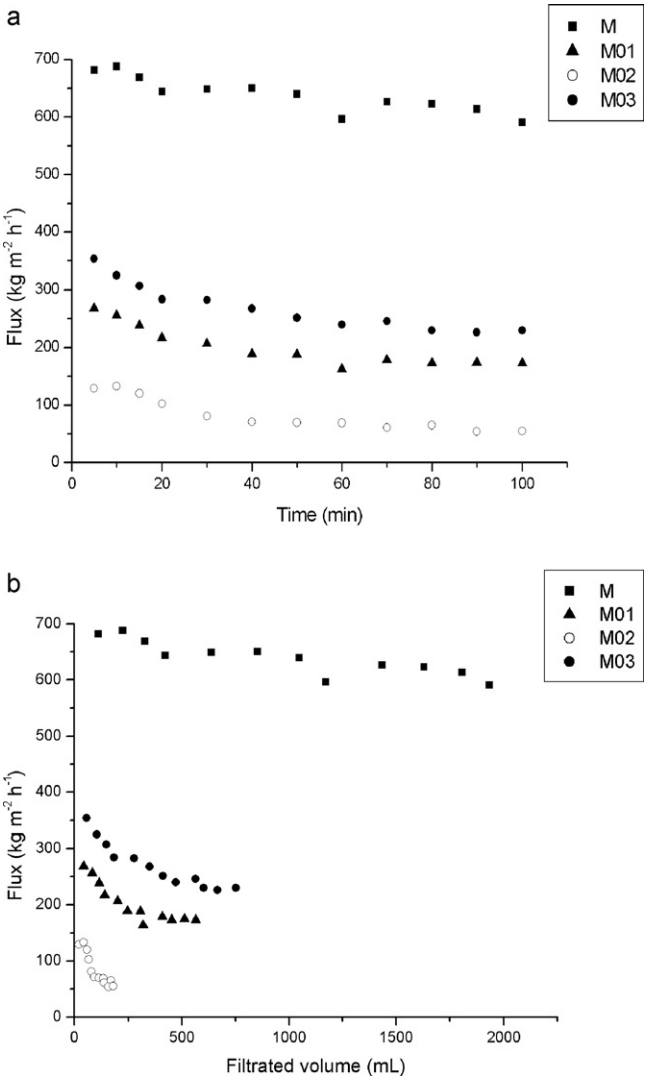

Fig. 6. Permeate fluxes of deionized water with clean membranes (step 1) as function of filtration time (a) and filtrated volume (b).

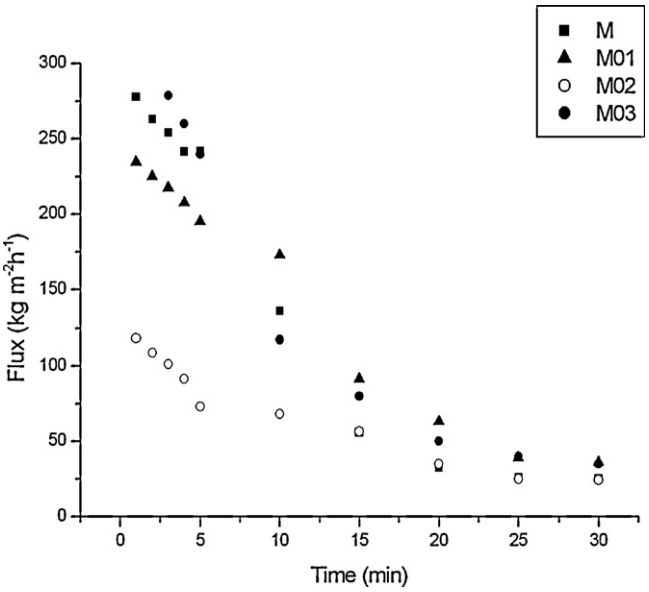

Fig. 7. Permeate fluxes of water contaminated with *E. coli* with all the proposed membranes before tap water filtration (step 2).

The permeate flux data of deionized water artificially contaminated with *E. coli* before tap water filtration (step 2 described in Section 2.3) is shown in Fig. 7.

Results presented in Fig. 7 show that there is a flux decline in the first 10 min of operation for both, modified and neat membranes, probably due to fouling occurrences related to the relative high bacteriological concentration. The flux behavior of the membranes M and M03 was similar during the filtration of water contaminated with *E. coli*, although the membrane M has presented higher fluxes during the filtration of pure deionized water. This behavior may be associated with the lower pore and cake resistance observed for the membrane M03, as soon as the lower fouling percent. Any way, as shown in Fig. 7, the stabilized flux was almost the same for the four tested membranes.

The obtained curves for the permeate flux of tap water (step 3 described in Section 2.3) for modified and neat membranes are presented in Fig. 8.

In this case, a pronounced flux decline is observed during the first 200 min of filtration for the membranes M, M01, and M03. It is important to notice that the initial fluxes for tap water filtration are higher than the last flux observed in the previous step (filtration of water contaminated with *E. coli*). This occurrence is due to the depressurization of the filtration module and also to its storage with deionized water after the filtration of water contaminated with *E. coli*. This procedure may have re-suspended the solids deposited onto the membrane surface.

Moreover, discontinuities are observed in the fluxes curves around 120, 240 and 360 min, for all the tested membranes. This behavior occurred because the experiments using tap water were divided into four assays of 120 min (2 h), and part of the material adhered on membrane surface was re-suspended during these pauses between the assays. These pauses were done in order to simulate a real utilization of a household filter.

The membranes M and M01 presented initial tap water fluxes (Fig. 8) quite similar to the fluxes observed with deionized water (Fig. 6). Contradictorily, during the beginning of the filtration (20 min), the membrane M03 presented higher fluxes with tap water than with deionized water. These initial points are probably related with some experimental dimness due to the destabilization of the system and membrane compression. The stabilized fluxes were taken into consideration for membrane comparisons.

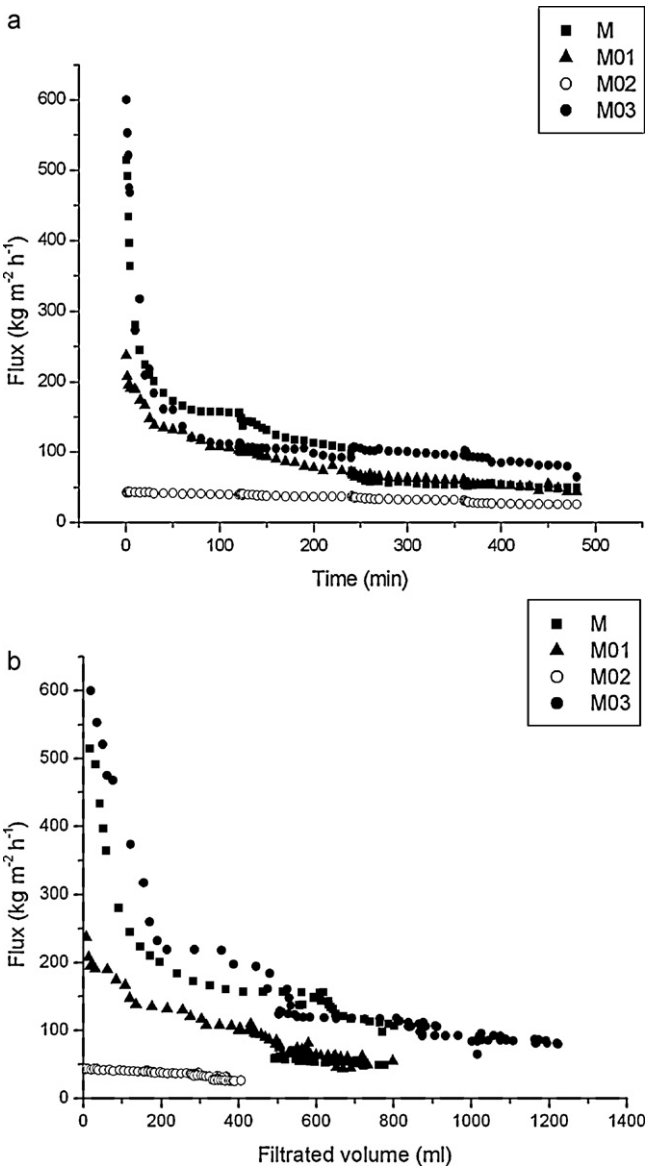

Fig. 8. Permeate fluxes of tap water with all the proposed membranes (step 3) as function of filtration time (a) and filtrated volume (b).

According to the obtained results, greater deposition times induces lower permeate fluxes. Fig. 8 shows that the membrane M02 presented the lowest permeate flux, especially at the beginning of the experiment. In this case, the highest deposition time (8 h) probably improved TiO_2 entrapment on the membrane surface, even with a low cathode current (0.35 A). Mansourpanah et al. [26] observed that the modification of polyethersulfone (PES)/polyamide (PI) blend membrane with TiO_2 enhanced Bovin Serum Albumin (BSA) fluxes. Anyway, Mansourpanah et al. [26] also observed that the deposition of TiO_2 at higher percentages decreased the permeate flux. Rahimpour et al. [10] showed that higher TiO_2 concentration in PES membranes decreased the flux of a solution containing milk and water. In fact, membrane material, as well as other factors, can affect overall hydrodynamic conditions, mainly due the chemical interaction between foulants and membrane. Damodar et al. [27] realized that membrane hydrophilicity also depends on how TiO_2 particles were spread over the membrane surface.

Fig. 8(b) presents the flux behavior of all the proposed membranes in relation to the filtrated volume of tap water. This figure

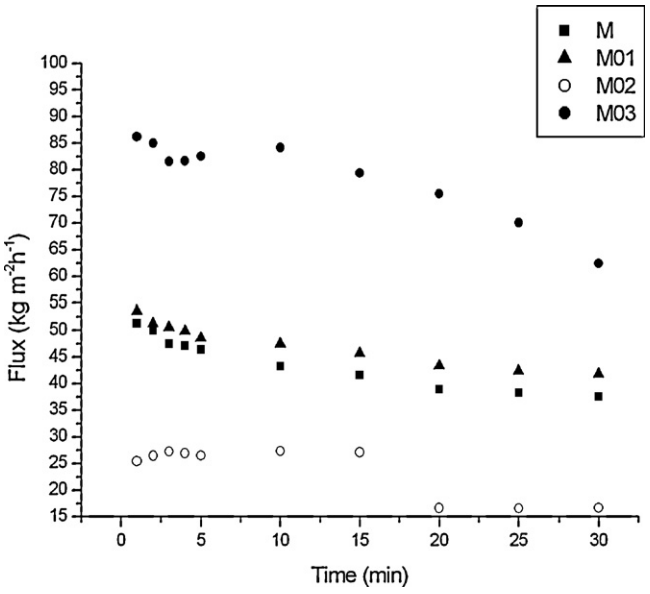

Fig. 9. Permeate fluxes of water contaminated with *E. coli* with all the proposed membranes after tap water filtration (step 4).

confirms the superior performance of the modified membrane M03, since it filtrate more tap water in 480 min of operation.

Fig. 9 shows the observed fluxes for deionized contaminated with *E. coli* after tap water filtration (step 4 described in Section 2.3). The observed fluxes are smaller than in the initial test (Fig. 7), as expected due to fouling occurrences. In this test, the membranes M and M01 presented similar flux results and the fluxes with the membrane M02 are the smallest one. The membrane M03 presented the highest flux behavior probably related to the smaller fouling and cake and pore blockage resistances due to the TiO_2 deposition at smaller time.

Fig. 10 presents deionized water fluxes with all the proposed membranes after the second bacteriological assay (step 5 described in Section 2.3). The membrane M03 presented the highest flux behavior for deionized water filtration through the fouled membrane. Even the membrane M02 presented flux values higher than the neat membrane M. These results show that the TiO_2 deposition on acetate cellulose membrane may improve the membrane utilization, since the observed fluxes are higher for the fouled modified membranes. However, the applied deposition time seems to be an important parameter to be optimized, since higher deposition times did not improve the membrane flux behavior.

Fig. 10(b) shows that, after its utilization, the membrane M03 was able to filtrate more deionized water than the other tested membranes.

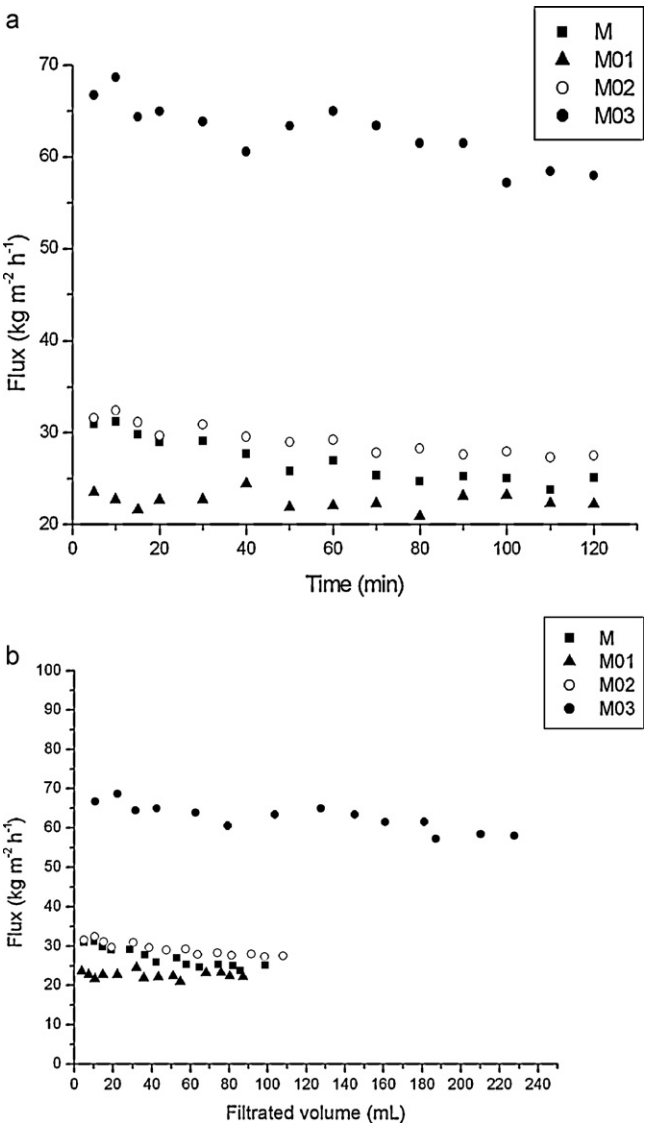

Fig. 10. Permeate fluxes of deionized water with fouled membranes (step 5) as function of filtration time (a) and filtrated volume (b).

3.3. Analyses of membrane resistances and fouling

Fouling percentages calculated by Eq. (2) and membrane resistances calculated following the resistance-in-series model are shown in Table 2.

Fouling percentage was lower for the modified membranes, especially for the membrane M02. Bae and Tak [15] also observed the fouling mitigation using TiO_2 deposited membranes, though TiO_2 did not play the role of photocatalyst.

Results presented in Table 2 show that the deposition of TiO_2 affected the membrane resistances. The hydraulic membrane resistance (R_m) increased for the membranes modified with TiO_2, as expected due to the deposition of a new layer onto the membrane surface. Rahimpour et al. [10] also observed that membrane resistance values (R_m) are higher for PES membranes coated with TiO_2 nanoparticles than for the neat one. This increase is more evident for the membrane M02, which was produced at the highest TiO_2 deposition time. Choi et al. [28] showed that an increase in the number of TiO_2 coating layers onto alumina membranes increase the filtration resistance. In general, the membrane M02 presented the smallest flux values. However, as the membrane M02 presented the smallest fouling percent, the flux of deionized water through the fouled M02 membrane is higher than through the membranes M and M01 (Fig. 10). The membrane M02 also presented the highest value for R_p, probably related to the higher deposition time (8 h), producing a membrane with tighter molecular weight cut-off (MWCO).

The membrane M01 presented the smallest value for R_p. This behavior is probably associated with the higher applied cathode current. This thermal energy reduces TiO_2 crystalization onto the membrane surface. On the other hand, the value of R_c for the membrane M01 is the highest one, showing that the pollutants present in the raw water formed a cake onto the membrane surface, although they have not internally blocked the membrane pore. This behavior contributes to a smaller decrease in the fouling percent related to the neat membrane (M).

Table 2
Resistances and % fouling calculated for neat and modified membranes.

Membrane	R_m (10^8 m^2 kg^{-1})	R_p (10^8 m^2 kg^{-1})	R_c (10^8 m^2 kg^{-1})	R_t (10^8 m^2 kg^{-1})	Fouling (%)
M	0.509	1.26	10.3	12.0	90.04
M01	1.73	0.586	11.4	13.7	87.36
M02	5.54	3.95	1.74	11.1	50.91
M03	1.33	1.12	2.74	5.19	74.34

The membrane M03 present the smallest increase in the R_m value related to the neat membrane and a decrease in R_p and R_c values. Generally, these results show that a smaller deposition time at a smaller cathode current ensures a smaller total membrane resistance. In this way, the antifouling property and long-term flux stability were enhanced using the membrane M03. Damodar et al. [27] also showed that the total resistance (R_t) is lower for the PVDF/TiO_2 membrane.

3.4. Impact of purification processes on water quality

Bacterial evaluations showed that membranes impregnated with TiO_2 did not decrease the *E. coli* removal, and, as expected, all the tested membranes (unmodified and modified) exhibited a bacteriological removal of 100% of the bacterium charge, both at the initial and at the final bacteriological assays (steps 2 and 4 described in Section 2.3).

The obtained pH values during tap water filtration were not substantially affected, as could be expected. During the operation with tap water the three evaluated membranes presented permeate pH values around 8.0.

According to the obtained results, all the tested membranes removed 100% of color during the tests with tap water. Since color-causing compounds are typically soluble this removal is probably associated with some adsorption process, rather than filtration.

Fig. 11 presents the turbidity reduction along the assays of tap water filtration with all the proposed membranes. The neat membrane (M) presented a more pronounced decline in turbidity reduction along the filtration time, from 89 to 62%. The modified membranes (M01 and M02) presented similar turbidity reductions around 76%, while the membrane M03 presented the lowest turbidity reduction, from 33 to 76%, at the beginning and at the end of the filtration, respectively. This low observed turbidity reduction of the membrane M03 is associated with the high flux and the low fouling percent. Since the studied process is a dead-end filtration, with no rejection, all the matter removed from the water must be deposited or incorporated to the membrane, increasing the fouling. In this way, the membrane M03 presented the smallest turbidity reduction and, consequently, the smallest fouling percent. Anyway the obtained turbidity value after the filtration with the membrane M03, ranging from 0.89 to 0.54 NTU, did not exceed the limit established by the WHO (1 NTU) [29].

Free chlorine removal is an important task for point-of-use filters, in order to remove disinfection byproducts with harmful long-term effects [30], as well as undesirable chlorine taste. In relation to free chlorine removal, the membranes M02 and M03 presented superior performance, with removal around 100% during all operation time with tap water, as presented in Fig. 12. The membrane M01 presented a decrease in free chlorine removal to less than 50% after 330 min of operation. The neat membrane (M) presented an inferior performance, around 45% of free chlorine removal after 450 min of operation. These results suggest that the TiO_2 deposition increased the chlorine removal capacity of the modified membranes. Due to the small chlorine particle size, chlorine removal may be related to reaction and/or adsorption processes, rather than filtration.

A longer deposition time inevitably induces a rougher surface, since the membrane substrate is replicated on the first monolayer and gradually increases with film thickness. A higher surface roughness enhances the surface area of the columnar crystalline grains; thus, the contact area between TiO_2 crystals and the pollutant is increased. The membranes M02 and M03 might outperforms the membrane M01 in relation to chlorine removal due to the atomic bombardment and the thermal energy transferred to the growing film, which is enhanced with a lower cathode current. This thermal energy will aid in adatom mobility, which in turn will enhance crystallisation and improve the efficiency of TiO_2. Additionally, the

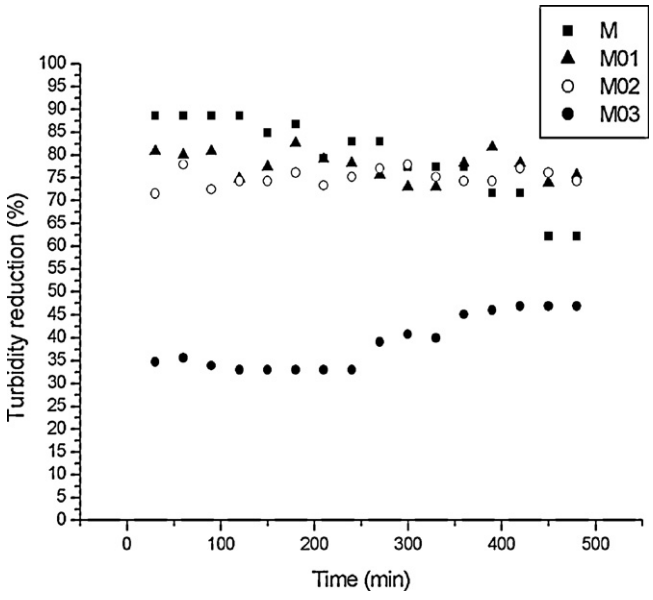

Fig. 11. Turbidity reductions in tap water after filtrations with all the proposed membranes.

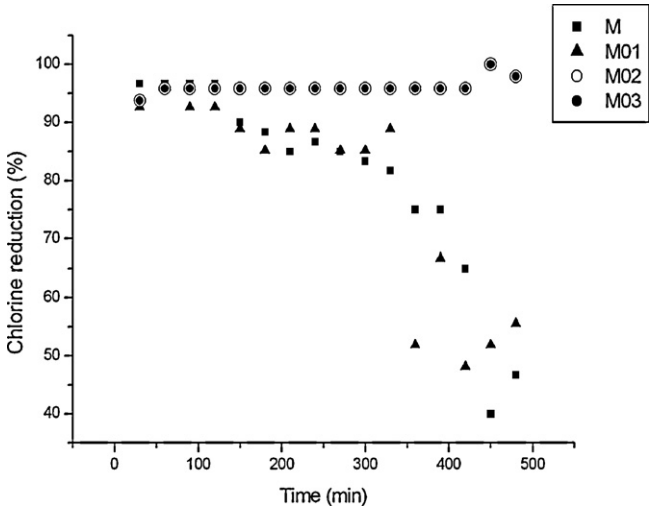

Fig. 12. Free chlorine removal in tap water after filtrations with all the proposed membranes.

higher the cathode current the higher the resputtering rate, which can lead to a lesser dense microstructure.

4. Conclusions

TiO_2 deposition on cellulose acetate membrane by the pulsed-frequency d.c. reactive magnetron sputtering method changed the filtration performance in a low-pressure apparatus for drinking water treatment.

The obtained results showed that TiO_2 deposition on membrane surface improves the water quality, especially in terms of turbidity and chlorine removals. The applied method for TiO_2 deposition is suitable for membrane morphology modification, mitigating the fouling effects, even without using the TiO_2 photocatalytic properties. Moreover, the proposed apparatus, without energy supply, can be considered as an alternative point-of-use treatment of water destined to human consumption.

Acknowledgments

Authors acknowledge to Conselho Nacional de Desenvolvimento Científico e Tecnológico (CNPq) and Fundação de Amparo à Pesquisa do Estado de Minas Gerais (FAPEMIG) for financial support.

References

[1] WHO – World Health Organization, Our Planet, Our Health, Geneva, 1992.
[2] T. Brick, B. Primrose, R. Chandrasekhar, S. Roy, J. Muliyil, G. Kang, Water contamination in urban south India: household storage practices and their implications for water safety and enteric infections, Int. J. Hyg. Environ. Health 207 (2004) 473–480.
[3] S.X. Tan, W.J. Zou, F.P. Jiang, S.Z. Tan, Y.L. Liu, D.S. Yuan, Facile fabrication of copper-supported ordered mesoporous carbon for antibacterial behavior, Mater. Lett. 64 (2010) 2163–2166.
[4] M. Peter-Varbanets, C. Zurbrugg, C. Swartz, W. Pronk, Decentralized systems for potable water and the potential of membrane technology, Water Res. 43 (2009) 245–265.
[5] H. Guo, Y. Wyart, J. Perot, F. Nauleau, P. Moulin, Low-pressure membrane integrity tests for drinking water treatment: a review, Water Res. 44 (2010) 41–57.
[6] H. Huang, K. Schwab, J.G. Jacangelo, Pretreatment for low pressure membranes in water treatment: a review, Environ. Sci. Technol. 43 (2009) 3011–3019.
[7] M. Peter-Varbanets, F. Hammes, M. Vital, W. Pronk, Stabilization of flux during dead-end ultra-low pressure ultrafiltration, Water Res. 44 (2010) 3607–3616.
[8] T. Clasen, J. Naranjo, D. Frauchiger, C. Gerba, Laboratory assessment of a gravity-fed ultrafiltration water treatment device designed for household use in low-income settings, Am. J. Trop. Med. Hyg. 80 (2009) 819–823.
[9] S.H. Kim, S.Y. Kwak, B.H. Sohn, T.H. Park, Design of TiO_2 nanoparticle self-assembled aromatic polyamide thin-film-composite (TFC) membrane as an approach to solve biofouling problem, J. Membr. Sci. 211 (2003) 157–165.
[10] A. Rahimpour, S.S. Madaeni, A.H. Taheri, Y. Mansourpanah, Coupling TiO_2 nanoparticles with UV irradiation for modification of polyethersulfone ultrafiltration membranes, J. Membr. Sci. 313 (2008) 158–169.
[11] W.Y. Wang, M.L. Yang, Y. Ku, Photoelectrocatalytic decomposition of dye in aqueous solution using Nafion as an electrolyte, Chem. Eng. J. 165 (2010) 273–280.
[12] S.S. Chin, T.M. Lim, K. Chiang, A.G. Fane, Factors affecting the performance of a low-pressure submerged membrane photocatalytic reactor, Chem. Eng. J. 130 (2007) 53–63.
[13] V. Likodimos, D. Dionysiou, P. Falaras, Clean water: water detoxification using innovative photocatalysts, Rev. Environ. Sci. Biotechnol. 9 (2010) 87–94.
[14] J. Kim, B. Van der Bruggen, The use of nanoparticles in polymeric and ceramic membrane structures: review of manufacturing procedures and performance improvement for water treatment, Environ. Pollut. 158 (2010) 2335–2349.
[15] T.H. Bae, T.M. Tak, Effect of TiO_2 nanoparticles on fouling mitigation of ultrafiltration membranes for activated sludge filtration, J. Membr. Sci. 249 (2005) 1–8.
[16] S.M. Marques, C.J. Tavares, L.F. Oliveira, A.M.F. Oliveira-Campos, Photocatalytic degradation of CI Reactive Blue 19 with nitrogen-doped TiO_2 catalysts thin films under UV/visible light, J. Mol. Struct. 983 (2010) 147–152.
[17] C.J. Tavares, S.M. Marques, S. Lanceros-Mendez, L. Rebouta, E. Alves, N.P. Barradas, F. Munnik, T. Girardeau, J.P. Riviere, N-doped photocatalytic titania thin films on active polymer substrates, J. Nanosci. Nanotechnol. 10 (2010) 1072–1077.
[18] C.J. Tavares, J. Vieira, L. Rebouta, G. Hungerford, P. Coutinho, V. Teixeira, J.O. Carneiro, A.J. Fernandes, Reactive sputtering deposition of photocatalytic TiO_2 thin films on glass substrates, Mater. Sci. Eng. B-Solid 138 (2007) 139–143.
[19] S.M. Marques, C.J. Tavares, S. Lanceros-Mendez, Z. Denchev, X-ray scattering experiments on sputtered titanium dioxide coatings onto PVDF polymers for self-cleaning applications, J. Appl. Polym. Sci. 119 (2011) 726–731.
[20] APHA, Standard Methods for the Examination of Water and Wastewater, Washington, 1998.
[21] A.I. Schafer, A.G. Fane, T.D. Waite, Nanofiltration—Principles and Applications, 1 ed., Elsevier Advanced Technology, Oxford, 2005.
[22] J.Y. Tian, Z.L. Chen, Y.L. Yang, H. Liang, J. Nan, G.B. Li, Consecutive chemical cleaning of fouled PVC membrane using NaOH and ethanol during ultrafiltration of river water, Water Res. 44 (2010) 59–68.
[23] M. Balakrishnan, M. Dua, P.N. Khairnar, Significance of membrane type and feed stream in the ultrafiltration of sugarcane juice, Separ. Sci. Technol. 36 (2001) 619–637.
[24] A.D. Syafei, C.F. Lin, C.H. Wu, Removal of natural organic matter by ultrafiltration with TiO_2-coated membrane under UV irradiation, J. Colloid Interface Sci. 323 (2008) 112–119.
[25] J.W. Lee, S.K. Tien, Y.C. Kuo, The effects of pulse frequency and substrate bias to the mechanical properties of CrN coatings deposited by pulsed DC magnetron sputtering, Thin Solid Films 494 (2006) 161–167.
[26] Y. Mansourpanah, S.S. Madaeni, A. Rahimpour, A. Farhadian, A.H. Taheri, Formation of appropriate sites on nanofiltration membrane surface for binding TiO_2 photo-catalyst: performance, characterization and fouling-resistant capability, J. Membr. Sci. 330 (2009) 297–306.
[27] R.A. Damodar, S.J. You, H.H. Chou, Study the self cleaning, antibacterial and photocatalytic properties of TiO_2 entrapped PVDF membranes, J. Hazard. Mater. 172 (2009) 1321–1328.
[28] H. Choi, E. Stathatos, D.D. Dionysiou, Sol-gel preparation of mesoporous photocatalytic TiO_2 films and TiO_2/Al_2O_3 composite membranes for environmental applications, Appl. Catal. B Environ. 63 (2006) 60–67.
[29] WHO – World Health Organization, Guidelines for drinking-water quality, Geneva, 2011.
[30] T.K. Nissinen, I.T. Miettinen, P.J. Martikainen, T. Vartiainen, Disinfection by-products in Finnish drinking waters, Chemosphere 48 (2002) 9–20.